Open Access

Research Article

Precis. Nanomed. 2026, 9(1):1771-1784

Irisin-Loaded Porous Silica Nanoparticles Enhance Bone Healing in High Cholesterol Diet-Induced Medaka Fish Model

Prashant Sadanandan[1,2], Silja Krishnan[3], Manzoor Koyakutty[3], and Manitha Nair[3*]

[1]*Department of Pharmaceutical Chemistry, Amrita School of Pharmacy, Amrita Vishwa Vidyapeetham, AIMS Health Sciences Campus, Kochi 682041, Kerala, India*

[2]*College of Pharmaceutical Sciences, Government Medical College Kottayam, Kerala University of Health Sciences, 686008, India*

[3]*Amrita School of Nanosciences and Molecular Medicine, Amrita Vishwa Vidyapeetham, AIMS Health Sciences Campus, Kochi 682041, Kerala, India*

Submitted: October 13, 2025 Accepted: March 6, 2026 Published: March 17, 2026

Graphical Abstract

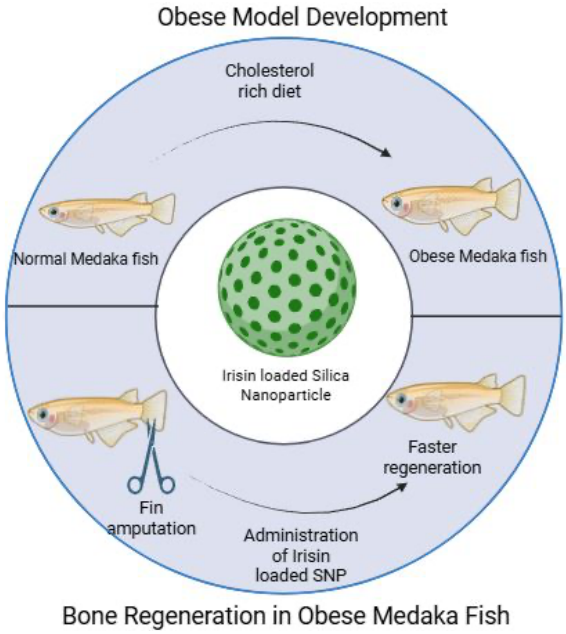

Abstract

Irisin is a myokine that stimulates browning of white adipocytes and enhances cortical bone mass during physical exercise. However, its short half-life limits its therapeutic potential, making sustained delivery systems desirable for bone tissue regeneration. In this study, we evaluated the effect of irisin-loaded porous silica nanoparticles (SiNPs) on caudal fin regeneration in a cholesterol-rich diet-induced obese medaka fish model, compared with irisin alone. Obese medaka were generated by feeding a 20% cholesterol diet for 2 months, followed by caudal fin amputation. Irisin formulations (free irisin or SiNP-loaded irisin at 350 ng and 700 ng) were administered via intraperitoneal injection. Cholesterol-fed medaka showed significant weight gain and fat accumulation over 30 days. Following fin amputation, bone regeneration was impaired in obese fish compared to normal controls. Notably, irisin-loaded SiNPs significantly enhanced fin regeneration, particularly at the higher dose (700 ng), compared to free irisin. These findings demonstrate that porous silica nanoparticle-mediated irisin delivery improves bone regeneration in an obese medaka fish model more effectively than irisin alone.

Keywords

Porous Silica Nanoparticles, Irisin, Bone Tissue Regeneration, Medaka fish Model

* Corresponding Author: Dr. Manitha B. Nair, manithanair80@gmail.com, manithanair@aims.amrita.edu

Purpose, Rationale, and Limitations

Obesity is associated with impaired bone healing due to chronic inflammation and reduced osteogenic potential. Although the myokine irisin promotes osteoblast activity and bone formation, its short half-life limits its therapeutic application. Therefore, this study aims to evaluate whether porous silica nanoparticles could provide sustained delivery of irisin and enhance bone regeneration in a cholesterol diet-induced obese Medaka fish model.

In this study, our objective was to evaluate the effect of irisin-loaded porous SiNP on caudal fin (bone) regeneration in a high-fat diet-induced obese medaka fish model. To our knowledge, this is the first report to show the outcome of nanoparticle-mediated irisin delivery on caudal fin regeneration in an obese medaka fish model.

The study also has some limitations, including a relatively small sample size and the use of a Medaka fish model. Therefore, further validation in mammalian models and detailed investigation of the molecular mechanisms underlying irisin-mediated bone regeneration are required.

Introduction

Obesity is a low-grade systemic chronic inflammatory state that predisposes to many metabolic diseases. Globally, more than 1.9 billion adults are overweight, and 650 million are obese [body mass index, BMI $\geq$ 30 kg/m^2] (1). Many studies report obesity as a risk factor for bone fractures and osteoporosis in humans (2). Adipose tissue accumulation elevates the levels of proinflammatory cytokines such as Tumor Necrosis Factor (TNF)-α, IL-1β, and IL-6, which activate osteoclast differentiation, resulting in bone resorption (3). Some of these cytokines downregulate the expression of genes such as RUNX2, osterix, and osteocalcin, thereby reducing osteoblast function and bone mass (4). During obesity, mesenchymal stem cells (MSCs) exhibit reduced osteoblast differentiation potential and increased adipogenesis (5). Hence, it is important to find a *therapeutic* approach to enhance bone union and regeneration in obese and overweight patients.

Physical exercise is considered a non-pharmacologic intervention to reduce body weight and enhance skeletal health. In response to exercise, the membrane protein FNDC5 (Fibronectin type III domain containing protein 5) is cleaved, releasing a small peptide called irisin, which can induce browning of white adipose tissue by upregulating the UCP1 gene (6). Irisin also promotes osteoblast proliferation and increases the expression of osteoblast-specific genes (7,8). Besides, it downregulates the expression of osteoclast differentiation marker genes, including receptor activators of *nuclear factor kappa B* (*NF-κB*), cathepsin K, and tartrate-resistant acid phosphatase (TRAP) (9). Intraperitoneal administration of recombinant irisin at a cumulative weekly dose of 100 µg kg^{-1} for 4 weeks increased trabecular and cortical bone and strength, whereas a higher irisin dose (3500 µg kg^{-1} per week) resulted in browning of adipose tissue in mice models (10). Even though irisin produces a *significant* positive impact on osteoblasts, it needs to be administered in multiple doses because of its short half-life. One promising approach is to use biodegradable nanoparticles that can release irisin in a sustained manner for a long period.

Many studies have shown that porous silica nanoparticles (SiNP) are biomimetic and biocompatible. Moreover, the biodegradability of porous silica makes it a good nanocarrier system from a translational perspective. Additionally, the porous structure allows high drug loading, and its mesopore volume/diameter can be tuned for efficient drug release (11,12). Biomedical application of silica in bone tissue engineering has also been demonstrated. In our lab, we have shown that a silica-containing HA-gelatin matrix can enhance endothelial and osteoblast cell function, resulting in vascularisation and new bone formation in a critical-sized rat femoral defect (13). Herein, mesoporous silica nanoparticles were used to deliver irisin *in vivo*. The medaka fish model (Oryzias latipes) was selected as an animal model because its bone biology mimics that of humans (14). Moreover, the skeleton component of medaka caudal fin can regenerate within a shorter period following tissue amputation through re-expression of sonic hedgehog (shh) and bone morphogenetic protein 2b pathway (15)

Preliminary viability and osteogenic differentiation studies were conducted using adipose-derived MSCs *in vitro* to select the drug concentration. Furthermore, two different irisin concentrations were loaded onto SiNPs, and their effects were evaluated *in vivo*.

Materials and Methods

In vitro cell culture studies

Preliminary studies were conducted using MSCs isolated from rat adipose tissue, with approval from the Institutional Animal Ethics Committee. The cells (20,000) were seeded into 96-well plates and maintained in α-minimal essential medium (α-MEM) with 10% fetal bovine serum (FBS) and 100 U/mL penicillin and streptomycin (Gibco, India) at 37°C and 5% CO_2. After 24 h, osteogenic supplements (10−8 M dexamethasone,10 mM β-glycerophosphate, and 0.05 mg mL−1 L-ascorbic acid) were added for the differentiation of MSCs into osteogenic lineage. Further, different concentrations of irisin (8880-IR-025, R&D, India) in phosphate-buffered saline (PBS) were added to the corresponding wells (75 ng/mL, 175 ng/mL, 350 ng/mL, 700 ng/mL) and incubated at 37°C. Cell morphology was observed using a phase-contrast microscope (Nikon ECLIPSE TE2000-U) after 24 h. Based on the result, an appropriate concentration range (175 ng/mL, 350 ng/mL, 700 ng/mL) was selected for viability and osteogenic differentiation studies.

Cell viability:

The viability of MSCs was quantified by lactate dehydrogenase (LDH) assay (Cytotox96 kit, Promega) on Days 1 and 7. For this, MSCs were lysed with 1% Triton X-100; the cell lysate (50 µL) was mixed with LDH substrate (50 µL), incubated at 37°C for 30 min, and then 0.1 M acetic acid was added to end the reaction, and the absorbance was measured at 492 nm (BiotekPowerklave XS). A calibration curve was generated by measuring LDH activity from lysates of known numbers of MSCs, allowing correlation between LDH activity and total cell number.

Osteogenic differentiation:

The osteogenic differentiation potential of MSCs was evaluated by alkaline phosphatase (ALP) activity on days 1, 7, and 14. Herein, the cell lysate (40 µL) was added to para-nitrophenyl phosphate (40 µL) (Sigma), incubated for 20 min at 37°C, and the absorbance was read at 405 nm (BioTek PowerWave XS). A calibration line was plotted using different concentrations of the ALP enzyme.

Irisin-loaded SiNP preparation and Release studies

Irisin Loading

Silica nanoparticles (SiNPs) were synthesized by the hydrolysis and condensation of tetraethyl orthosilicate (TEOS) following a modified Stöber method (16,17). Briefly, 100 mL of ethanol (80% v/v) was mixed with ammonium hydroxide (3 mL, 28%, Alfa Aesar) and cetyltrimethylammonium bromide (CTAB, 1.5 mg/mL; Spectrochem) and stirred for 30 min at room temperature. TEOS (Sigma-Aldrich) was added dropwise, and the reaction was stirred continuously until a stable colloidal suspension was obtained.

The nanoparticles were collected by centrifugation at 12,000 g for 15 min, washed repeatedly with absolute ethanol and deionized water (Millipore), and dried. CTAB was removed by calcination at 550 °C, yielding porous SiNPs.

For irisin loading, porous SiNPs were dispersed in 1× PBS and incubated with irisin peptide solutions at two initial doses (350 ng and 700 ng), maintaining a nanoparticle-to-irisin weight ratio of 1:1. Irisin solution was added dropwise to the SiNP suspension and incubated at 4 °C under mild stirring for 1 h to facilitate adsorption. Following incubation, irisin-loaded SiNPs were separated by centrifugation and washed with deionized water to remove unbound peptide.

The amount of unbound irisin present in the supernatant and wash solutions was quantified using a bicinchoninic acid (BCA) protein assay. A standard calibration curve was prepared using known concentrations of irisin, and absorbance was measured at 562 nm. The concentration of irisin in the supernatant was calculated from the calibration curve. The irisin loading efficiency (%) was calculated using the following equation:

$$\text{Irisin loading efficiency (\%)} = \frac{(\text{Total irisin added} - \text{Irisin in supernatant})}{\text{Total irisin added}} \times 100$$

Physicochemical Characterization

The size and morphology of silica nanoparticles (SiNPs) were evaluated by transmission electron microscopy (TEM; Tecnai G2, FEI, USA) operated at an accelerating voltage of 200 kV. Particle size analysis was performed using the image analysis software (Gatan Microscopy Suite Version 2.11.1408.0) associated with the instrument on low-magnification micrographs covering approximately 6.25 μm^2. For each sample, 80–100 nanoparticles were randomly selected to determine the mean particle diameter, and the standard deviation was calculated from the corresponding size distribution. The functional groups of the nanoparticles were also analyzed by Fourier transform infrared (FTIR) spectroscopy (PerkinElmer Spectrum RX-1) over the spectral range of 4000–500 cm^{-1}. For this, the nanoparticle samples were mixed with potassium bromide, compressed into pellets, and subsequently analyzed.

Release Studies

For release studies, irisin-loaded nanoparticles were suspended in 1 mL PBS (pH 7.4) at 37˚C (n=3). At each predetermined time point (days 1 and 5), the nanoparticle suspension was centrifuged at 10,000 × g at 37°C for 10 min, and the supernatant containing the released irisin was collected. The concentration of irisin in the supernatant was determined using the Human Irisin ELISA Kit (Sigma-Aldrich Co.) according to the manufacturer's instructions. A calibration curve was plotted using a known irisin concentration.

Obese model development and characterisation

Male adult Japanese medaka fish (QURT Strain) (2 months post-fertilization) were chosen for the study after obtaining approval from the Institutional Animal Ethics Committee. All animals used in the study were maintained under an environment involving a 14:10–h light/dark cycle at 28°C ± 2, pH (6.8-7.4) at a controlled re-circulation system. After the acclimatization period of 1 week, medaka fish were divided into two dietary groups (Normal diet and cholesterol-rich diet) (N=4). They received their respective diets for 8 weeks (4 fish per 2 L tank). Medaka fish in the normal diet group were fed with commercially available powder feed (Otohime B2) (40 mg/fish/day). High-cholesterol feed was prepared by soaking egg yolk in a diethyl ether solution containing cholesterol (20% cholesterol), which was mixed with Otohime B2 and was given four times per day.

BMI determined obesity in medaka fish on days 0, 30, and 60. BMI was calculated by dividing the body weight (g) by the square of the body length (cm)] (18). Moreover, adipose tissue accumulation was evaluated on days 30 and 60 by staining with borondipyrromethene (BODIPY) (Sigma-Aldrich). For this, the medaka fish was anaesthetised using 0.02% Tricaine methanesulfonate (MS-222, Sigma-Aldrich); stained with 1 µg BODIPY for 1 h in the dark at 28°C, and observed under a fluorescent microscope (Leica MSV269 Fluorescence stereo microscope, Germany) with excitation and emission filters of 480 and 520, respectively.

Caudal fin amputation and characterisation

Normal and obese medaka fish were anaesthetised using 0.02% Tricaine methane sulfonate (MS-222, Sigma-Aldrich). Further, six bony rays at the ventral half of the caudal fin (~3 mm) (below the proximal bony ray bifurcation) were amputated with a scalpel blade (19) (n=4). Animals were injected with 10 µL irsin (drug alone and nanoparticle-loaded drug) intraperitoneally using a Hamilton microsyringe. PBS was used in the normal group. Animals were then placed in separate tanks and maintained under a controlled environment as described above. Seven groups of animals were included in the study (a) Normal fish with bone defect: NF (b) Obese fish with bone defect: OF (c) Obese fish injected with irisin at low concentration (350 ng): IrL (d) Obese fish injected with irisin at high concentration (700 ng): IrH (e) Obese fish injected with SiNP-irisin (350 ng): Si-IrL (f) Obese fish injected with SiNP-irisin (700 ng): Si-IrH (g) Obese fish injected with SiNP alone: SiN.

An increase in fin regeneration was measured using a bright-field microscope on days 3 and 6 following anaesthesia. The length of six fin rays was measured from the plane of amputation to the distal tip of each bony ray using Image J software, and the average distance was recorded.

Fluorescence imaging of fluorescein isothiocyanate labelled SiNPs in medaka

Fluorescein isothiocyanate (FITC) labelled SiNPs (FITC-SiNPs) were prepared as previ-

ously described(20). Briefly, an equimolar solution of FITC (Fluorescein Isothiocyanate, Sigma) in ethanol and aminopropyltriethoxysilane (APTES, Alfa Aesar) was stirred for 48 h to get a yellowish silane core. This silane core was mixed with an equal volume of TEOS, precipitated in ethanol (100 mL, 90% v/v), and homogenized with 1 mL NH_4OH. The reaction was stirred for 24 h at room temperature to obtain a colloidal solution, which was then washed with absolute ethanol and deionized water to yield FITC-SiNPs.

The nanoparticles were dispersed in PBS (1mg/mL) and ultrasonicated for 2 min using a 2 mm diameter probe at 20 % amplitude (VCX 130, Sonics Vibra Cell. 10 µL of the dispersion was injected intraperitoneally into anaesthetised male adult medaka (n=2). At 24 h post-injection, the fish were imaged under a fluorescent microscope (EVOS M5000, Invitrogen, USA) to observe the distribution of the particles *in vivo*.

Statistical Analysis

One-way analysis of variance (ANOVA) was employed to assess the statistical significance. A *p*-value less than 0.05 was considered significant for all analyses. All experiments were expressed in terms of mean ± standard deviation.

Results

In vitro cell culture studies

The effect of different irisin concentrations (75 ng, 175 ng, 350 ng, and 700 ng) on MSC morphology was initially assessed. All the cells in the group exhibited spindle-shaped morphology. An increased population doubling time was observed in cells with irisin, and this effect was more pronounced at concentrations ranging from 175 ng to 700 ng compared with cells without irisin (Fig. 1). Based on this study, 75 ng was omitted from further studies.

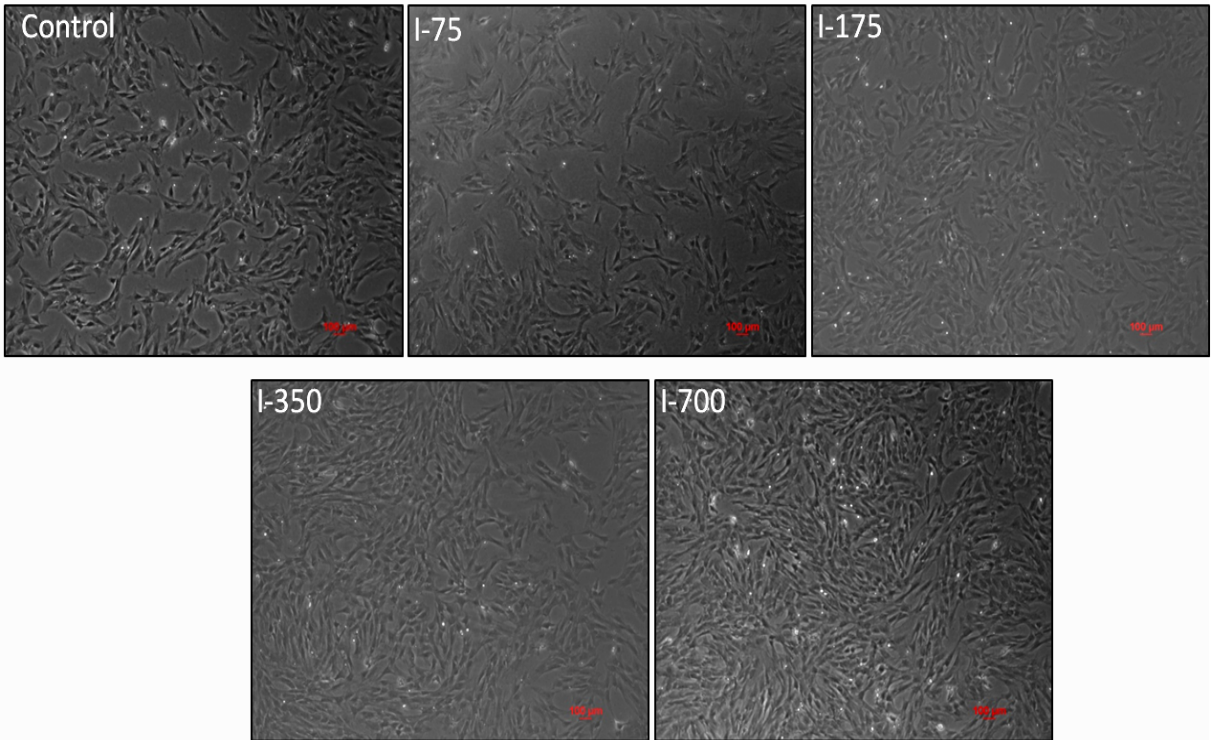

Fig. 1: Phase-contrast images of MSCs treated with irisin at 24 h (Scale bar: 100µm). The cell number was increased with increasing concentration of irisin

The viable cell number was quantified by the LDH assay over 7 days. There was a time-dependent increase in cell numbers across all groups. Irisin treatment, mainly I-350 and I-700, significantly enhanced cell viability on Days 1 and 7. There were 5-10-fold more viable cells in those groups than in cells without irisin (Fig. 2A). To evaluate osteogenic differentiation, an ALP assay showed increased activity in irisin-treated groups. The highest enzyme activity was observed on Day 7 in the irisin groups,

whereas in the control groups it was delayed until the second week. During comparison, ALP activity was significantly higher in the I-350 and I-700 groups than in the control and I-175 groups on day 7. However, there was no difference in enzyme activity on day 1 and day 14 among the groups (Fig. 2B). Since irisin at 350 and 700 ng showed higher ALP activity, indicating enhanced early osteogenic commitment, these concentrations were selected for loading onto silica nanoparticles and for subsequent in vivo studies.

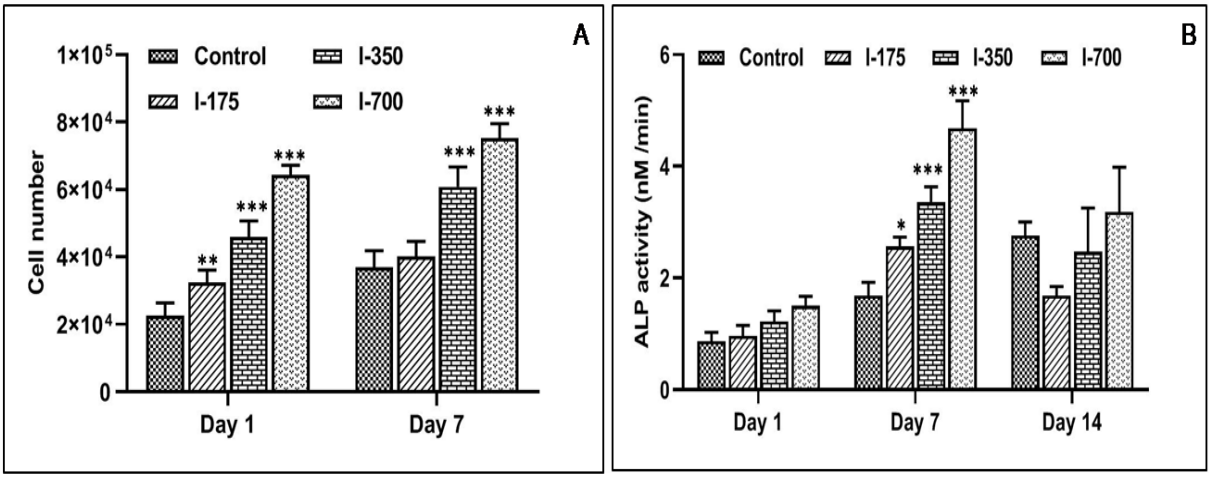

Fig. 2: Effect of irisin on osteogenic cells (A) Cell viability (B) Osteogenic differentiation. The cellular response viability was significantly enhanced in the presence of Irisin when compared to control (- p<0.05, ** - p< 0.01, *** - p <0.001)*

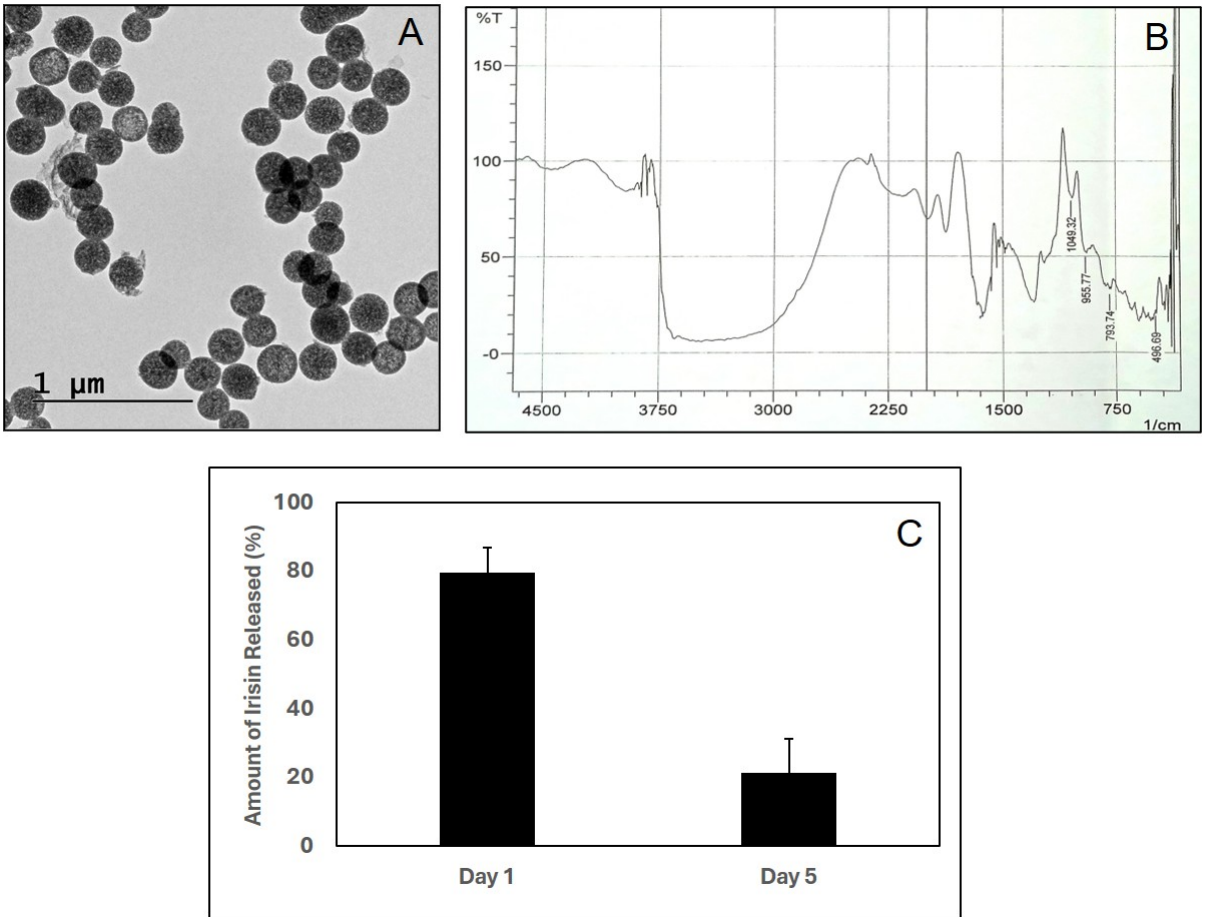

Fig. 3: (A) TEM image of irisin-loaded porous SiNPs, (B) FTIR spectrum, (C) irisin release percentage. 700 ng irisin-loaded porous SiNP were used for the study

Irisin Release from Porous SiNP

Porous silica nanoparticles were synthesized and loaded with irisin. TEM analysis revealed that the SiNPs were spherical and monodispersed, with an average particle size of 200 ± 50 nm (Fig. 3).

FTIR spectroscopy of the silica nanoparticles showed characteristic peaks of Si–O–Si stretching at ~1080 cm^{-1} (asymmetric) and ~800 cm^{-1} (symmetric), and a bending vibration at ~470 cm^{-1}. A broad band at ~3430 cm^{-1} and a weak peak at ~1630 cm^{-1} corresponded to surface –OH groups and adsorbed water, confirming the formation of porous silica nanoparticles with intact siloxane bonds. However, irisin–silica interactions could not clearly be resolved by FTIR.

The irisin loading efficiency was approximately 50%, determined by measuring the unbound peptide in the supernatant using a BCA assay. Further, irisin release kinetics were evaluated by ELISA. A burst release of ~80% was observed on Day 1. By Day 5, approximately 20% of the loaded irisin was released, corresponding to a concentration of 149 ± 70 ng, which was relevant to the timing of subsequent *in vivo* experiments.

Characterization of the Obese Medaka Fish Model

The medaka fish were fed a normal or cholesterol-rich diet and assessed for obesity over 8 weeks. Body weight increased over time in the normal diet group, but the increase was not statistically significant. However, in the high-cholesterol diet group, body weight was almost twice that of the control group from Day 30 onwards. The body weight on Day 60 was noticeably higher than on Day 30. Furthermore, BMI was calculated as body weight (g) divided by the square of body length (cm). There was a significant increase in BMI in the high-cholesterol diet group on Day 30, which reached a peak on Day 60 ($p < 0.001$) (Fig. 4).

The high-cholesterol diet-fed medaka fish group exhibited an enlarged belly. BODIPY staining revealed increased lipid droplet deposition in the abdominal region in those groups. The belly size increased from Day 30 to 60 (Fig. 5).

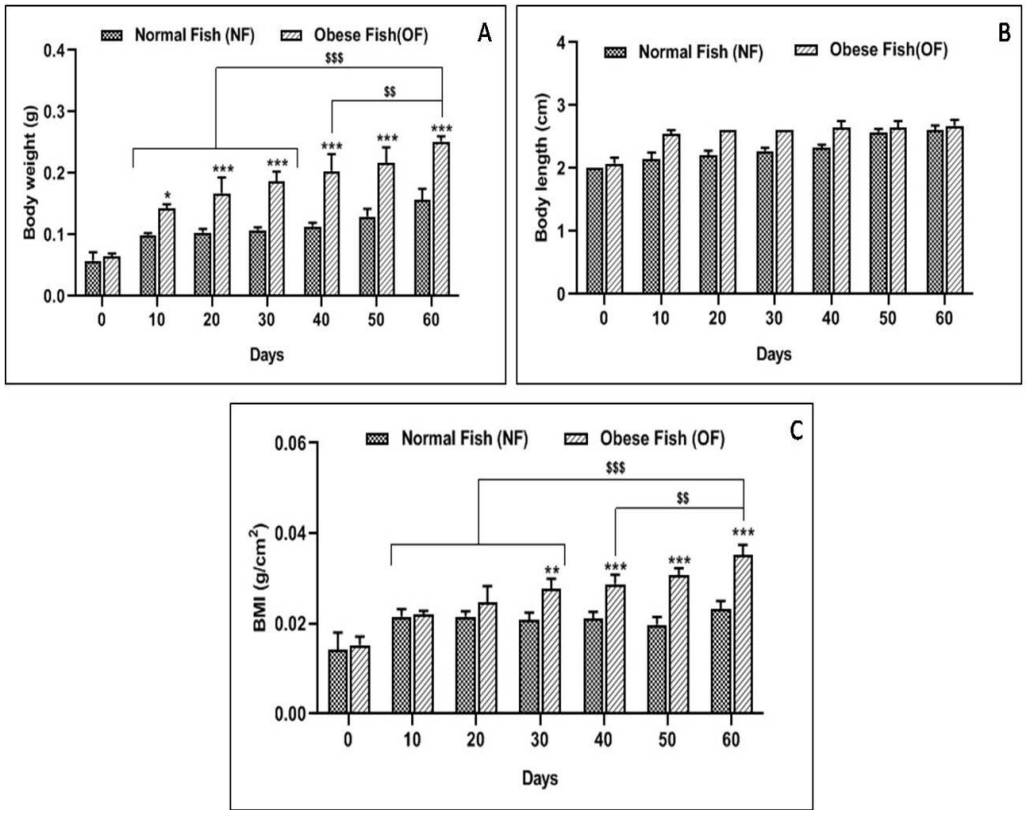

Fig. 4: Evaluation of body weight (A), Body length (B), and BMI (C) in Medaka fish fed with normal and high-cholesterol diet for 60 days (n=4). There was a significant increase in body weight and BMI in cholesterol diet-fed groups than in normal groups from the 2nd week (- p<0.05, *** - p<0.0001). Also, body weight and BMI of cholesterol diet-fed groups on day 60 were higher than those on other days ($$ - p<0.01, $$$ - p<0.001)*

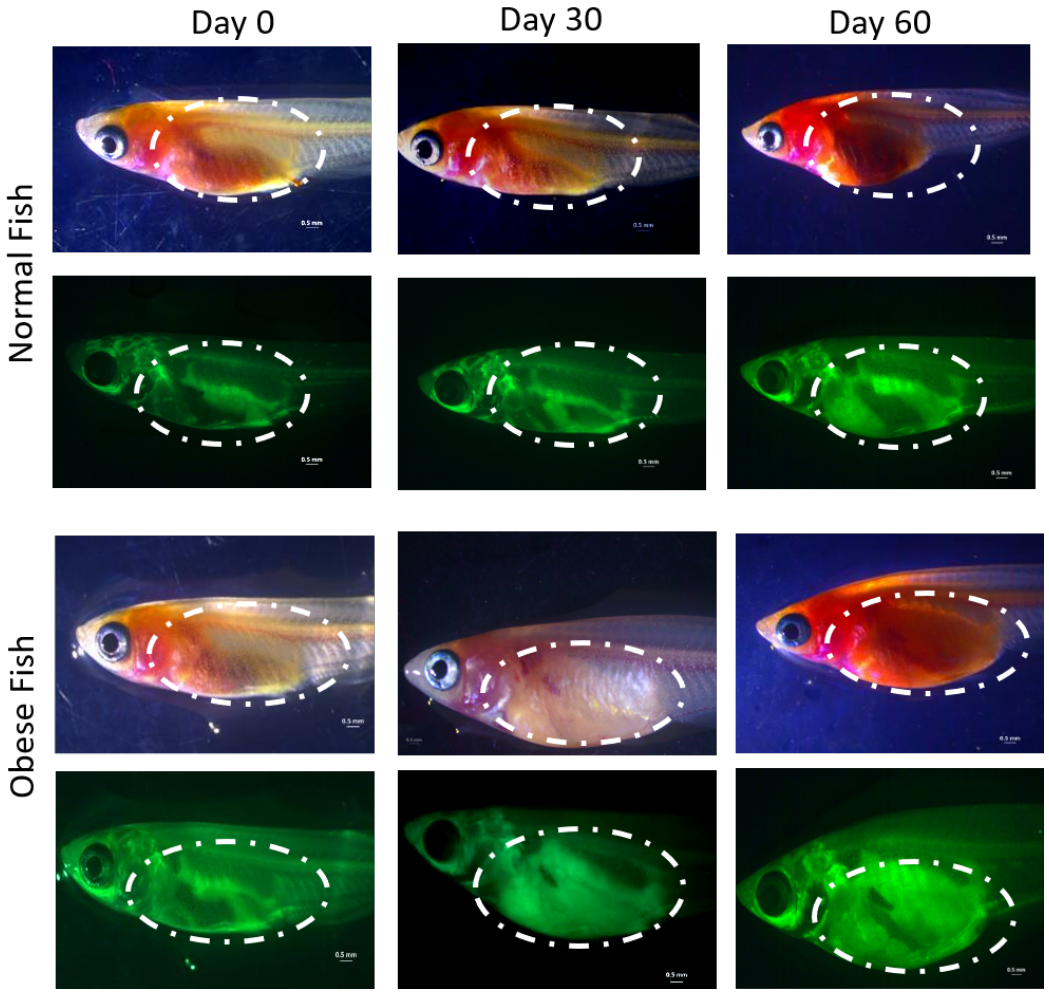

Figure 5: Evaluation of adipose tissue in medaka fish fed with normal and high-cholesterol diet for 60 days. Upper panel: Stereo microscopic images; Lower panel: Fluorescent images of fish stained with Bodipy stain. Scale bar: 0.5 mm

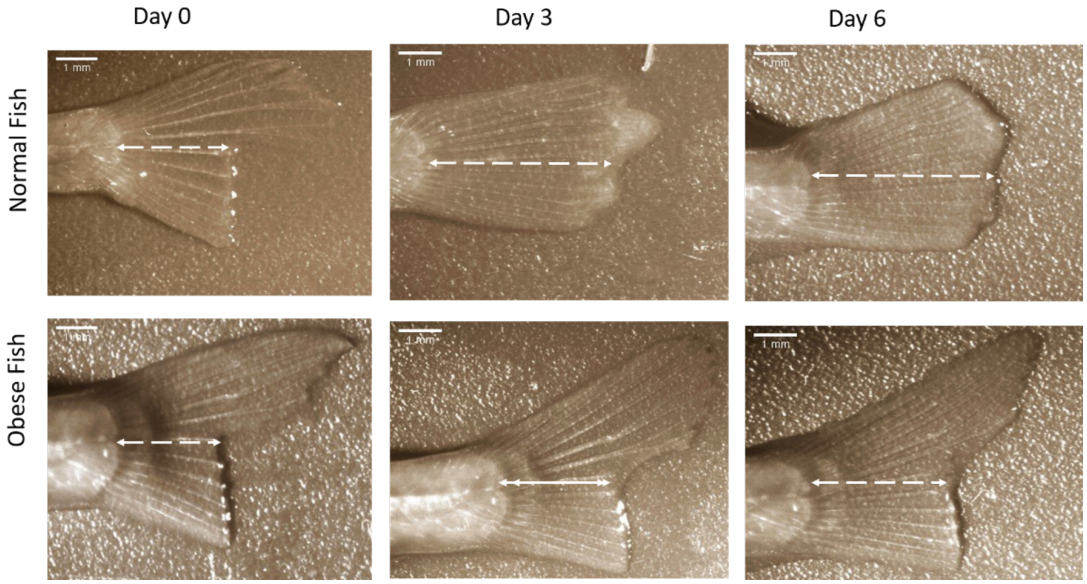

Figure 6: Evaluation of caudal fin regeneration in normal and obese medaka fish at Day 0, 3, and 6 post amputations (Bright-field images). Arrows indicate the length of regenerated bone (Scale bar: 1 mm)

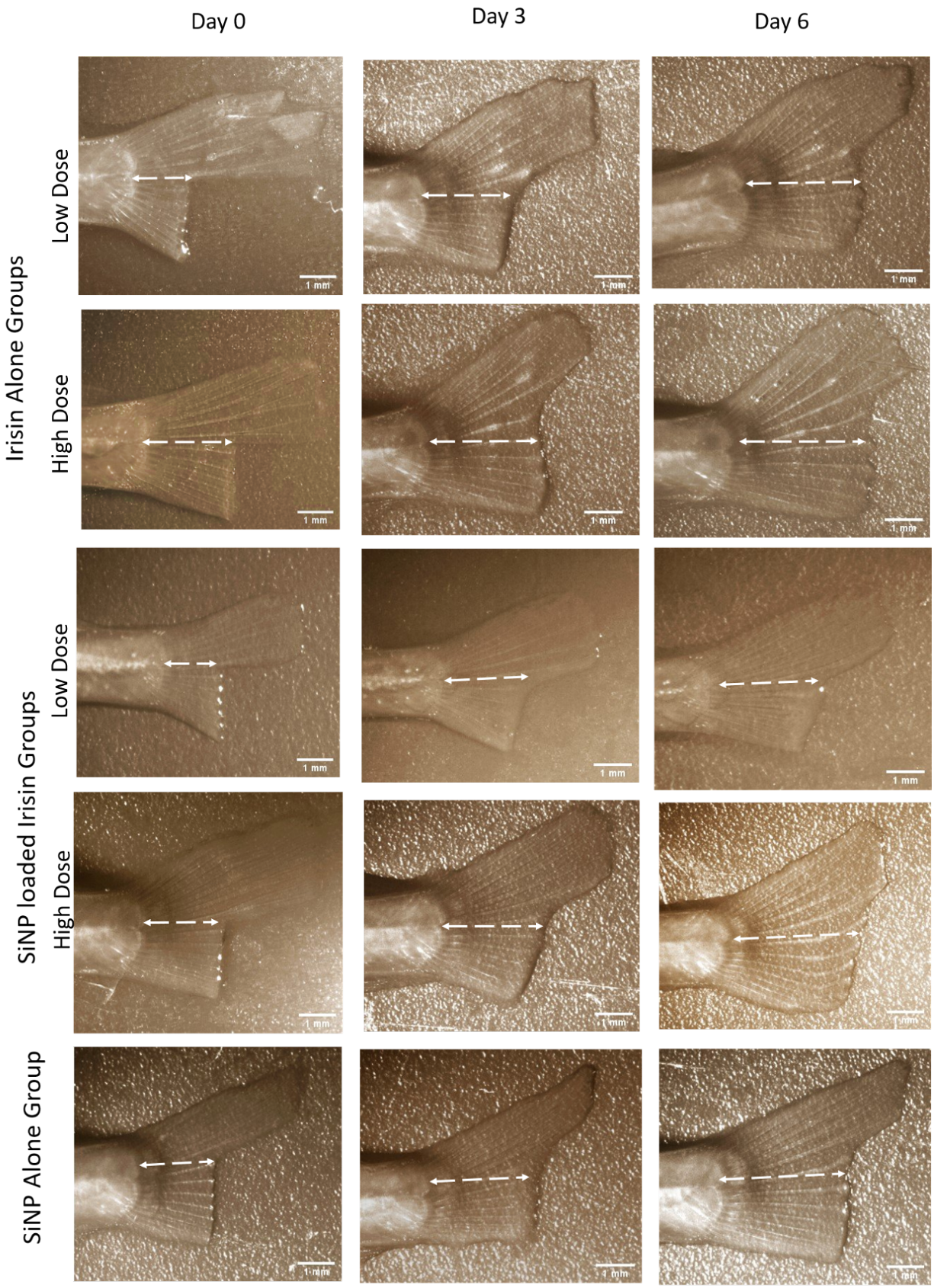

Fig. 7: Evaluation of caudal fin regeneration in obese medaka fish injected with irisin at low and high doses (Bright-field images). Arrows indicate the length of regenerated bone (Scale bar: 1 mm)

Caudal Fin Amputation and Characterisation

In this part, caudal fin amputation was created in obese medaka fish [Six bony rays below the proximal bifurcation] and injected with irisin intraperitoneally (irisin alone and silica nanoparticle-irisin conjugate at low and high doses). Further, the length of tissue regeneration was measured between 0 and 6 days post amputation (dpa). The results showed that the length of regenerated bone in obese fish was shorter than that in normal fish at 3 and 6 dpa (Fig. 6). This suggests that high-cholesterol-induced obesity impairs caudal fin regeneration in medaka. When irisin was injected, there was better bone growth in obese fish at a higher dose (700 ng), especially on Day 6. The pattern of regenerated bone was similar to bone segments located proximal to the amputation plane (old bone). However, complete regeneration was not achieved in any of the 6 bony rays.

Quantitatively, irisin-loaded SiNP showed greater tissue regeneration on days 3 and 6. Silica nanoparticles alone were injected and also affected bone tissue regeneration, similar to the IrL groups (Figs. 7,8).

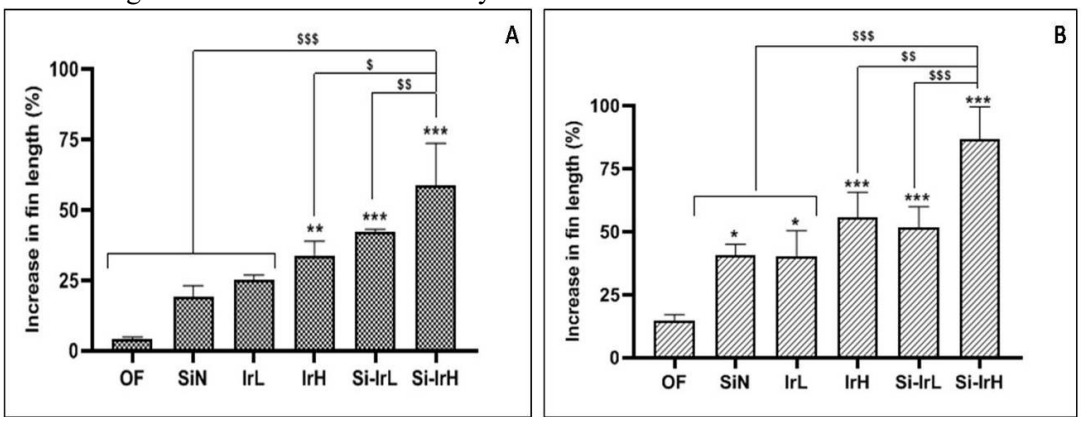

Fig. 8: The percentage of regenerated caudal fin on Day 3 (A) and Day 6 (B) post amputation. The regenerated fin was statistically significant in irisin-treated groups in comparison to those without treatment (- p<0.05, ** - p<0.01, *** - p < 0.001). The highest regeneration was seen in Si-IrH with respect to other treated groups ($ - p<0.05, $$ - p<0.01, $$$ - p < 0.001)*

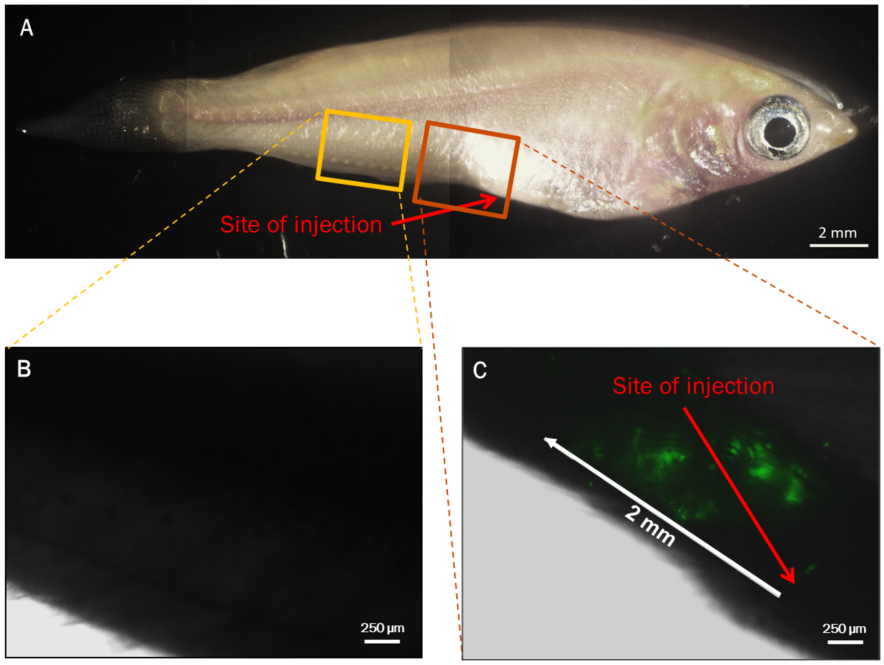

Fig. 9: Fluorescence imaging of FITC-SiNPs in male medaka. (A) Bright-field stereo microscopic image of an adult male medaka. Superimposed images of the region around the site of injection (C) and the posterior region of the fish (B), 24 hours post-injection.

The FITC-SiNPs were observed to have traversed around 2 mm from the site of injection towards the posterior end when observed under the fluorescent microscope 24 hours post-injection. No evidence of particles was observed further towards the posterior region, particularly near the tail fins (Fig. 9). This may be due to higher bone density in the region, which can limit penetration and affect the sensitivity of signal capture at the site.

Discussion

Intraperitoneal injection of irisin causes adipose tissue browning along with an increased cortical bone mass (6), but the half-life of irisin is short. Hence, a delivery system that slowly releases the drug at the site of action might be a strategy to improve therapeutic efficacy. Mesoporous silica nanoparticles exhibit high drug-loading capacity and sustained release properties, as their size can be tuned (20,21). In this study, our objective was to evaluate the effect of irisin-loaded SiNP on caudal fin regeneration in a cholesterol-rich diet-induced obese medaka model, compared with irisin alone. For this, 200 nm-sized SiNPs were used.

As a preliminary step, the effects of different irisin doses (75 ng, 175 ng, 350 ng, 700 ng) on MSC viability and osteogenic differentiation were assessed over 2 weeks. Osteogenic differentiation was evaluated based on ALP activity, an early marker of osteoblasts (22). The results showed that both cell viability and osteogenic differentiation were enhanced in the presence of irisin compared to the control. This was similar to previous reports, wherein irisin promoted proliferation and differentiation of osteoblasts and increased the expression of RUNX2 (Runt-related transcription factor 2) and osx (osteoblastic transcription regulators) (9). Besides, Colaianni *et al.* found that the conditioned media collected from myoblasts of exercised mice could enhance osteoblast differentiation *in vitro* (23). Osteoblasts and MSCs express receptors for irisin, which act in an autocrine manner to regulate bone cell function. However, herein, the maximum cell response was obtained at a concentration of 350–700 ng, whereas in other studies, recombinant irisin at 100 ng/mL has shown beneficial effects (3). This may be due to the different cell types used in both experiments (adipose-derived stem cells versus MC3T3-E1).

For *in vivo* studies, obesity was induced in adult medaka fish model, as it is a simple and inexpensive animal model. Moreover, a high-fat diet induced in medaka and zebrafish mimics several features of human metabolic syndrome, including abdominal obesity, hypertriglyceridemia, low levels of HDL cholesterol, and hyperglycemia. Most of these studies compared normal and obese animals by overfeeding adult zebrafish with artemia or flakes ("natural" diet). In a few studies, a cholesterol-rich diet was given, but the fat content varied. In one report, adult zebrafish fed a high-cholesterol diet (4%) for 12 weeks developed hypercholesterolemia (24). Adult medaka fed with 56.7% fat developed obesity-related glomerulopathy (25). Landgraf *et al*. aimed to establish a protocol (zebrafish fed 60 mg artemia versus 5 mg artemia and egg yolk powder containing 59% fat) for using zebrafish as a model of obesity-related metabolically healthy versus metabolically unhealthy adipose tissue accumulation (26). After 8 weeks, both groups showed increased body weight and adipose tissue mass compared to the control group. But high-fat-fed zebrafish also exhibit metabolic alterations, including hyperglycemia, ectopic lipid accumulation in the liver, and a metabolically unhealthy visceral adipose tissue depot. Based on this report, a similar protocol was followed in our study, with slight modifications to induce obesity: adult medaka fish were fed 20% cholesterol along with commercially available powder feed for 8 weeks.

In practice, the male medaka fish model helps establish obesity. The body weight and BMI of female fish are higher than those of male fish, as the former regularly produce eggs that contain large amounts of lipids (27). Moreover, ovaries in adult female fish can account for up to 29% of body weight compared to 2% for the testis in male zebrafish (28). Because of this, body weight measurement in adult female fish does not reflect adipose tissue accumulation but may also indicate oocyte growth. Hence, male medaka fish were selected for the study and fed a normal or cholesterol-rich diet for 8 weeks. There was an increase in body weight and in the cholesterol-fed group as days increased. Fat deposition was observed mainly in the abdominal region, as confirmed by BODIPY staining. (Obese zebrafish: A small fish for a major human health condition). Further, BMI

was calculated and found to be 1.4-fold higher in high-fat diet-induced groups after Day 30. Previous studies have reported that fat deposits in the abdominal viscera and a superior BMI (< 1.1-fold) confirm obesity in fish models (18).

Further, caudal fin amputation was done in medaka fish [Six bony rays below the proximal bifurcation] as it represents a good model to study bone regeneration. The caudal fin *skeleton* is simple, easily accessible for surgery, and possesses better r*egenerative ca*pability (29). The fin is composed of several segmented bony fin rays, each of which is composed of a pair of concave hemirays that surround connective tissue, including fibroblasts, MSCs, and osteoblasts (30). The stages of caudal fin regeneration occur in three sequential phases: (i)a thin layer of epithelial cell formation within 24 h, (ii) MSCs proliferate to form blastema within 48-72 h (a proliferative mass of progenitor cells), and (iii) intramembranous bone outgrowth and mineralization within a week (31). Herein, the amputated fish were injected with irisin (alone and silica nanoparticle-loaded irisin at low and high doses). Bright-field images demonstrated that the length of regenerated bone segments in obese fish was shorter when compared to those of normal fish. This was similar to earlier studies in obese mouse models. It is reported that levels of growth factors such as calcitonin gene-related peptide (CGRP), fibroblast growth factor, and transforming growth factor-β1 were low in obese mice, which delays fracture healing (32). Interestingly, there was increased fin regeneration in irisin-loaded at high doses, especially using silica nanoparticles. In the irisin-loaded SiNP group, drug release lasted nearly 5 days (as confirmed by drug release studies), thereby enhancing tissue regeneration. In contrast, in the irisin-alone group, the drug may have been retained at the site of action for a shorter period. However, SiNP should be modified to control the initial burst release and sustain release for a longer period to enable its application in large animal models.

Conclusion

The present study evaluated the effect of irisin-loaded porous SiNP on caudal fin (bone) regeneration in a cholesterol-rich diet-induced obese medaka fish model, compared with irisin alone. When the caudal fin was amputated, the tissue regeneration was slower in obese fish when compared to normal fish. Interestingly, increased bone regeneration was achieved with the administration of irisin-loaded silica nanoparticles at a higher concentration. In summary, we demonstrated a simple SiNP-mediated drug-delivery approach to enhance tissue regeneration in obese models.

Author Contributions: P.S. and S.K. designed and performed the experiments, analyzed the data, and prepared the manuscript. M.N. and M.K. conceptualized the study, supervised the research and experimental design, and critically reviewed the manuscript. All authors have read and approved the final version of the manuscript.

Funding: Financial support for this work came from the Department of Science and Technology, Government of India (M. Tech grant Number: KH.NS.P2MLM18001).

Acknowledgments: The authors gratefully acknowledge the support of Amrita Vishwa Vidyapeetham for providing the research facilities required for this work. The authors also thank Mr. Sajin P. Ravi and Ms. Arya Raju for their technical assistance with the TEM experiments.

Conflicts of Interest: The authors declare no conflict of interest. The funders had no role in the study's design, data collection, analysis, or interpretation, manuscript writing, or decision to publish the results. For requests, write to the journal office: editor@precisionnanomedicine.com.

Quote this article as Prashant Sadanandan, Silja Krishnan, Manzoor Koyakutty, and Manitha Nair, Irisin-loaded Porous Silica Nanoparticles Enhance Bone Healing in High Cholesterol Diet-induced Medaka Fish Model. Precis.nanomed, 9(1)1771-1784, https://doi.org/10.33218/001c.159028.

References

1. Drabińska, N., Wiczkowski, W., & Piskuła, M. K. (2021). Recent advances in the application of a ketogenic diet for obesity management. *Trends in Food Science & Technology*, 110, 28-38.
2. Colaianni, G., Brunetti, G., Faienza, M. F., Colucci, S., & Grano, M. (2014). Osteoporosis and obesity: Role of Wnt pathway in human and murine models. *World journal of orthopedics*, 5(3), 242.
3. Cao, J. J. (2011). Effects of obesity on bone metabolism. *Journal of orthopaedic surgery and research*, 6(1), 30.
4. Roy, B., Curtis, M. E., Fears, L. S., Nahashon, S. N., & Fentress, H. M. (2016). Molecular mechanisms of obesity-induced osteoporosis and muscle atrophy. *Frontiers in physiology*, *7*, 439.
5. Hu, L., Yin, C., Zhao, F., Ali, A., Ma, J., & Qian, A. (2018). Mesenchymal stem cells: cell fate decision to osteoblast or adipocyte and application in osteoporosis treatment. *International Journal of Molecular Sciences*, *19*(2), 360.
6. Boström, P., Wu, J., Jedrychowski, M. P., Korde, A., Ye, L., Lo, J. C.& Spiegelman, B. M. (2012). A PGC1-α-dependent myokine that drives brown-fat-like development of white fat and thermogenesis. *Nature*, *481*(7382), 463-468.
7. Qiao, X., Nie, Y., Ma, Y., Chen, Y., Cheng, R., Yin, W., & Xu, L. (2016). Irisin promotes osteoblast proliferation and differentiation via activating the MAP kinase signaling pathways. *Scientific reports*, *6*(1), 18732.
8. Chen, Z., Zhang, Y., Zhao, F., Yin, C., Yang, C., Wang, X., & Qian, A. (2020). Recombinant irisin prevents the reduction of osteoblast differentiation induced by stimulated microgravity through increasing β-catenin expression. *International journal of molecular sciences*, 21(4), 1259.
9. Ma, Y., Qiao, X., Zeng, R., Cheng, R., Zhang, J., Luo, Y.,& Xu, L. (2018). Irisin promotes proliferation but inhibits differentiation in osteoclast precursor cells. *The FASEB Journal*, *32*(11), 5813-5823.
10. Colaianni, G., Cuscito, C., Mongelli, T., Pignataro, P., Buccoliero, C., Liu, P.,& Grano, M. (2015). The myokine irisin increases cortical bone mass. *Proceedings of the National Academy of Sciences*, *112*(39), 12157-12162.
11. Nair, A., Greeny, A., Nandan, A., Sah, R. K., Jose, A., Dyawanapelly, S., & Sadanandan, P. (2023). Advanced drug delivery and therapeutic strategies for tuberculosis treatment. *Journal of Nanobiotechnology*, *21*(1), 414.
12. Greeny, A., Nair, A., Sadanandan, P., Satarker, S., Famurewa, A. C., & Nampoothiri, M. (2024). Epigenetic alterations in Alzheimer's disease: impact on insulin signaling and advanced drug delivery systems. *Biology*, *13*(3), 157.
13. Menon, Deepthy, Koyakutty, M., Mohan, C. C., Nair, S. V., & Nair, M. B. (2017). Bioinspired Composite Matrix Containing Hydroxyapatite-Silica Core-Shell Nanorods for Bone Tissue Engineering. *ACS Applied Materials & Interfaces*, *9*(32), 26707-26718.
14. Lin, C. Y., Chiang, C. Y., & Tsai, H. J. (2016). Zebrafish and Medaka: new model organisms for modern biomedical research. *Journal of biomedical science*, *23*(1), 19.
15. Quint, E., Smith, A., Avaron, F., Laforest, L., Miles, J., Gaffield, W., & Akimenko, M. A. (2002). Bone patterning is altered in the regenerating zebrafish caudal fin after ectopic expression of sonic hedgehog and bmp2b or exposure to cyclopamine. *Proceedings of the National Academy of Sciences*, *99*(13), 8713-8718.
16. Wang, J., Teng, Z., Tian, Y., Fang, T., Ma, J., Sun, J.,& Lu, G. (2013). Increasing cellular uptake of mesoporous silica nanoparticles in human embryonic kidney cell line 293T cells by using lipofectamine 2000. *Journal of biomedical nanotechnology*, *9*(11), 1882-1890.
17. Stöber, W., Fink, A., & Bohn, E. (1968). Controlled growth of monodisperse silica spheres in the micron size range. *Journal of colloid and interface science*, *26*(1), 62-69
18. Yuniarto, A. (2019). Zebra fish model of obesity: Relevance to metabolic syndrome. *International Journal of Green Pharmacy*, *13*(2).
19. Sekimizu, K., Tagawa, M., & Takeda, H. (2007). Defective fin regeneration in medaka fish (Oryzias latipes) with hypothyroidism. *Zoological science*, *24*(7), 693-699.

20. Wang, Y., Sun, Y., Wang, J., Yang, Y., Li, Y., Yuan, Y., & Liu, C. (2016). Charge-reversal APTES-modified mesoporous silica nanoparticles with high drug loading and release controllability. *ACS applied materials & interfaces*, *8*(27), 17166-17175.
21. Sadanandan, P., Payne, N. L., Sun, G., Ashokan, A., Gowd, S. G., Lal, A., & Koyakutty, M. (2022). Exploiting the preferential phagocytic uptake of nanoparticle-antigen conjugates for the effective treatment of autoimmunity. *Nanomedicine: Nanotechnology, Biology and Medicine*, *40*, 102481.
22. Douglas, T. E., Vandrovcová, M., Kročilová, N., Keppler, J. K., Zárubová, J., Skirtach, A. G., & Bačáková, L. (2018). Application of whey protein isolate in bone regeneration: Effects on growth and osteogenic differentiation of bone-forming cells. *Journal of Dairy Science*, *101*(1), 28-36.
23. Colaianni, G., Cuscito, C., Mongelli, T., Oranger, A., Mori, G., Brunetti, G., & Grano, M. (2014). Irisin enhances osteoblast differentiation *in vitro*. *International journal of endocrinology*, (1), 902186.
24. Han, B., Kou, S., He, K., Han, Y., Wang, Y., Huang, T., & Ye, X. (2018). Anti-hypercholesterolemic effect of berbamine isolated from Rhizoma Coptidis in hypercholesterolemic zebrafish induced by high-cholesterol diet. *Iranian Journal of Pharmaceutical Research: IJPR*, *17*(1), 292.
25. Ichimura, K., Kawashima, Y., Nakamura, T., Powell, R., Hidoh, Y., Terai, S., & Obara, T. (2013). Medaka fish, Oryzias latipes, as a model for human obesity-related glomerulopathy. *Biochemical and biophysical research communications*, *431*(4), 712-717.
26. Landgraf, K., Schuster, S., Meusel, A., Garten, A., Riemer, T., Schleinitz, D., & Körner, A. (2017). Short-term overfeeding of zebrafish with normal or high-fat diet as a model for the development of metabolically healthy versus unhealthy obesity. *Bmc Physiology*, *17*(1), 4.
27. Zang, L., Maddison, L. A., & Chen, W. (2018). Zebrafish as a model for obesity and diabetes. *Frontiers in cell and developmental biology*, *6*, 91.
28. Li, J., & Ge, W. (2020). Zebrafish as a model for studying ovarian development: Recent advances from targeted gene knockout studies. *Molecular and Cellular Endocrinology*, *507*, 110778.
29. Cardeira, J., Gavaia, P. J., Fernández, I., Cengiz, I. F., Moreira-Silva, J., Oliveira, J. M.,& Laizé, V. (2016). Quantitative assessment of the regenerative and mineralogenic performances of the zebrafish caudal fin. *Scientific Reports*, *6*(1), 39191.
30. Lebedeva, L., Zhumabayeva, B., Gebauer, T., Kisselev, I., & Aitasheva, Z. (2020). Zebrafish (Danio rerio) as a model for understanding the process of caudal fin regeneration. *Zebrafish*, *17*(6), 359-372.
31. Poss, K. D., Shen, J., Nechiporuk, A., McMahon, G., Thisse, B., Thisse, C., & Keating, M. T. (2000). Roles for Fgf signaling during zebrafish fin regeneration. *Developmental biology*, *222*(2), 347-358.
32. Gao, F., Lv, T. R., Zhou, J. C., & Qin, X. D. (2018). Effects of obesity on the healing of bone fracture in mice. *Journal of orthopaedic surgery and research*, *13*(1), 145.